XLVI CILAMCE
VITÓRIA - ES - BRAZIL - 2025
XLVI IBERO-LATIN AMERICAN CONGRESS ON COMPUTATIONAL METHODS IN ENGINEERING

# Neural network model for determining the critical bending moment of web-tapered beams

Marissa T. Silva[1], João V. F. Dias[1]

[1]*Dept. of Civil Engineering, Federal University of Espírito Santo*
*Avenida Fernando Ferrari, No. 514, 29075-910, Espírito Santo/Vitória, Brazil*
*marissa.t.silva@edu.ufes.br, joao.v.dias@ufes.br*

**Abstract.** In the design of web-tapered members, determining the critical bending moment is a complex task since the non-prismatic geometry of the members leads to difficulties in their stability analysis. This paper proposes a neural network regression model to obtain the critical bending moment of web-tapered members. A database of 15,000 critical bending moment values for different profile geometries was generated through numerical analyses to train and evaluate the neural network models. The model was developed using the Adam optimizer and the influence of predictor variables was examined. The findings suggest that the use of both geometric and slenderness parameters as input variables increases the model's performance. The proposed model achieved a mean average percentage error of approximately 3% in predicting the critical bending moment. Finally, the model predictions were compared with a formulation from the literature. A significant improvement in prediction accuracy was observed using the regression model compared to the considered equations.

**Keywords:** web-tapered members, critical bending moment, neural networks, machine learning, steel structures.

## 1 Introduction

Web-tapered members are a structural solution characterized by varying cross section along its span and are generally subjected to bending [1]. These profiles provide great strength and stiffness with minimum weight, resulting in optimal geometry. Compared to prismatic members, they may lead to material savings, as deeper sections can be used in regions with high bending moments and thicker webs in areas of high shear stress. Additionally, they offer more fabrication flexibility, as a wide variety of profiles can be produced with a minimum inventory of different plates and coils [2].

In general, structural standards do not provide a specific formulation for calculating of the critical moment of web-tapered members, which discourages their use. The Brazilian standard [3] establishes usage requirements that underestimate the load-bearing capacity of these members, as it considers the cross-sections with the most unfavorable characteristics for each verification parameter in the design of the structures, disregarding the influence of sections of higher inertia and lower slenderness along the member's length on the behavior of the structure. The European standard [4] presents a general method and a type of second-order analysis that can be applied to web-tapered members but does not establish formulations for critical buckling loads. The American standard [5] does not provide a specific calculation method for the analysis and design of web-tapered members. However, it indicates the AISC Design Guide 25 [2] as a reference for their flexural strength approach and second-order analysis.

Determining the critical bending moment of web-tapered members is a complex task, as their non-prismatic geometry leads to difficulties in their stability analysis. Several studies have adopted a finite element method (FEM) approach for the study of the problem [6-8]. However, only a few have proposed analytical expressions for its determination. In this context, machine learning (ML) is an alternative for determining critical moments of web-tapered members, due to its ability to efficiently handle challenging tasks. ML has been widely adopted in

the field of structural engineering for parameter prediction [9-13].

Braham and Hanikenne [7] developed a method for lateral-torsional buckling (LTB) verification of web-tapered beams, in which the critical moment is given by eq. (1), where $I_{zf}$ is the transverse moment of inertia of the compressed flange of the beam, $L_{LT}$ is the lateral buckling length, $t_{f1}$ and $t_{f2}$ are the thicknesses of the beam's flanges, $d_{eq}$ is the equivalent web depth, simplified as $d_{eq} = (d_1 + d_2)/2$. This method was compared with numerical simulations, limited to beams with trapezoidal webs, equal and constant flanges, linear bending moment distribution, and without local buckling or cross-sectional distortion.

$$M_{cr} = \frac{\pi^2 E I_{zf}}{L_{LT}^2}\left(d_{eq} + \frac{t_{f1}}{2} + \frac{t_{f2}}{2}\right). \tag{1}$$

Raftoyiannis and Adamakos [14] proposed critical moment modification factors for different tapering ratios of I-beams subjected to LTB, based on numerical analysis. For simply supported beams, it was found that the critical moment decreases as the tapering ratio increases. Kováč [15] applied the Rayleigh-Ritz method to modify two differential equations originally developed by Vlasov for web-tapered members subjected to LTB. The equations were validated through a parametric study and subsequently verified using Ansys. Asgarian et al. [16] investigated both theoretical and numerical models for the stability of thin-walled beams subjected to LTB, providing estimates of buckling loads. The results were compared with Ansys numerical simulations, showing relative errors lower than 1% in most cases. Trahair [17] presented a procedure for determining the critical moment of continuous or braced beams, considering the moment distribution along the member, the tapering ratio, and the effects of restraints between segments. The solutions proved to be conservative or close to the accurate results obtained through finite element analysis. Couto [18] developed an artificial neural network (ANN) model for calculating the critical bending moment of prismatic and web-tapered beams, mono-symmetric and doubly-symmetric. Simply supported beams subjected to major-axis bending were analyzed.

As an alternative to previously adopted approaches, this research proposes an ANN regression model for determining the critical buckling bending moment of web-tapered beams. To this end, a numerical database of 15,000 samples was created through simulations on Ansys. The model results were compared with a literature formulation. Furthermore, this study also aims to develop a classifier that predicts the most critical buckling mode of the members and explores its influence on the regression model.

# 2 Methodology

The methodology adopted in this work consisted of two main phases: data generation and development of machine learning models. First, a database composed of critical bending moment values obtained through numerical simulations was created. Then, this data was used to train a K-Nearest Neighbors (KNN) classifier for determining the beams' buckling mode and to develop regression models to predict either the critical bending moment or the stresses in the beams. The following section details the steps taken to develop the numerical models and to implement the KNN classifier and the ANN regression model.

## 2.1 Numerical modeling

The database used to train the ML models consisted of 15,000 numerical models generated through Ansys, with parametric control over the geometry of the structure. Each model represented a simply supported web-tapered beam, tapered on both the top and bottom edges of the web, and with constant flange and web thickness along its span. Four groups of cross-sectional depths were considered: 0.300, 0.600, 0.900 and 1.200 m. The SHELL181 element was used to simulate the surfaces of the web and flanges of the beam, while MPC184 was employed to model the boundary conditions. These rigid elements simulated fork supports on both ends of the beam. Concentrated moments were applied at both ends. Figure 1 presents the typical geometry of the model, along with its boundary and loading conditions, and the typical buckling mode for profiles subject to LTB. In order to obtain a structured mesh, the element size was standardized to $b_f/8$ in both directions for all area elements of the structure, where $b_f$ is the flange width of the cross-section.

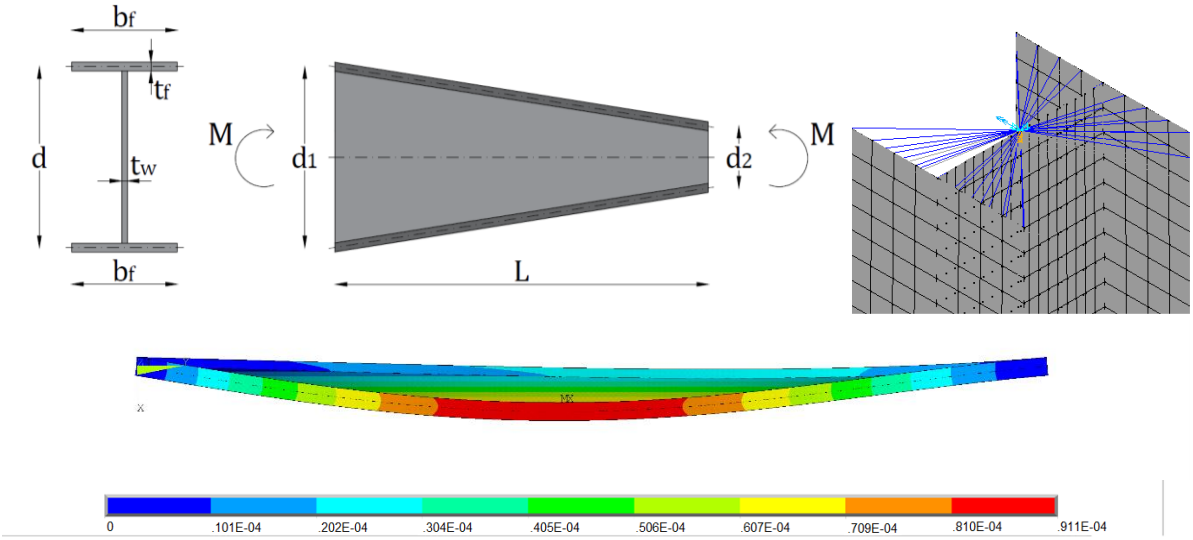



Figure 1. Typical geometry, boundary conditions, loading conditions and buckling mode (LTB) of the model

### 2.2 KNN Classifier Development

To define the KNN classification model, a total of 954 visually labeled data from the original database of 15,000 models was used, 550 corresponding to the Web Local Buckling (WB) class, 381 to the Lateral Torsional Buckling (LTB) class, and 23 to the Web Flange Buckling (FB) class. The data was divided so that 15% of the total was allocated to the test set. The number of neighbors investigated was in the range of 1 to 7. Web slenderness, flange slenderness, slenderness for lateral-torsional buckling verification and maximum-to-minimum depth ratio were considered input features of the model, as they are directly associated with the buckling mode of the beam. To evaluate the classifier's performance, the recall, precision, and F1-score metrics were analyzed. Once this model was established, the KNN classifier was applied to the remaining unlabeled portion of the dataset (14,046 samples), assigning a category to each instance. As a result, the dataset consisted of 9,119 WB samples, 117 FB samples, and 5,764 LTB samples. Subsequently, two types of regression were trained, one that disregards the class label and uses all samples regardless of buckling mode, and one separate regression for each class of buckling mode class.

### 2.3 ANN Development

Aiming to develop the ANN model, the dataset was randomly divided into training and test sets, corresponding to 80% and 20% of the total data, respectively. The training set was further randomly split into training (75%) and validation (25%) subsets. The Adam optimizer was employed due to its ability to handle problems with large volumes of data and a high number of parameters [19]. The default learning rate of 0.001 was adopted. Considering the wide range of magnitudes of the critical bending moment data, the Mean Absolute Percentage Error (MAPE) was defined as the loss function of the ANNs. The Mean Absolute Error (MAE), Mean Squared Error (MSE), and MAPE were used to measure the models' performance.

In order to find the best ANN architecture for the prediction problem, a hyperparameter tuning procedure was conducted. A grid search technique was applied for different combinations of number of layers, neurons per layer, and activation functions. The architecture consisting of three hidden layers, with 83 neurons per layer and the ReLU activation function was selected, since it demonstrated the best performance without compromising the computational cost of the model.

Once the model architecture was defined, the influence of the input features was analyzed using four different versions of the ANN. The input features taken into account were span length ($L$), flange width ($b_f$), flange thickness ($t_f$), web thickness ($t_w$), maximum cross-sectional depth ($d_1$), minimum cross-sectional depth ($d_2$), flange slenderness ratio ($r_1 = b_f/t_f$), web slenderness ratio at the maximum cross-sectional depth ($r_2 = d_1/t_w$),

global slenderness ($\lambda_{FLT} = L/r_y$, where $r_y$ is the radius of gyration about the y-axis), and moment of inertia about the x-axis at the minimum ($I_{x,min}$) and maximum ($I_{x,max}$) cross sections. Table 1 summarizes the input features considered in each version. The first version includes only geometric features. In the second version, these values were replaced by slenderness ratios. The third version combines both types of parameters. Finally, the fourth version also considers the moment of inertia about the x-axis, in addition to the parameters described in the third version. All versions include the cross-section depths at both ends as parameters, allowing the identification of beams with different tapering ratios.

Table 1. Input features for each version of the 83/83/83/1 architecture

| Version | Input features |
|---|---|
| 1 | $L$, $b_f$, $t_f$, $t_w$, $d_1$, $d_2$ |
| 2 | $r_1$, $r_2$, $\lambda_{FLT}$, $d_1$, $d_2$ |
| 3 | $L$, $b_f$, $t_f$, $t_w$, $d_1$, $d_2$, $r_1$, $r_2$, $\lambda_{FLT}$ |
| 4 | $L$, $b_f$, $t_f$, $t_w$, $d_1$, $d_2$, $r_1$, $r_2$, $I_{x,min}$, $I_{x,max}$ |

# 3 Results and Discussion

This section presents the findings regarding the performance of the classification and ANN models, the effects of data classification on the regression models, and a comparison between the regression models and existing formulas reported in the literature.

## 3.1 Classification Model Performance

The trained classifiers with 4 and 6 neighbors provided the best results in terms of accuracy (0.94) and macro averages, indicating more consistent performance, as shown in Tab. 2. The 4-neighbor classifier reported higher precision for the WB class (0.98) compared to the 6-neighbor classifier (0.97). Since the WB is the more representative in the dataset, the 4-neighbor classifier was selected for training the regression model.

Table 2. Macro average performance of classification models by number of neighbors

| No. of neighbors | Precision | Recall | F1-score |
|---|---|---|---|
| 1 | 0.94 | 0.84 | 0.88 |
| 2 | 0.94 | 0.84 | 0.88 |
| 3 | 0.94 | 0.95 | 0.95 |
| 4 | 0.95 | 0.96 | 0.96 |
| 5 | 0.94 | 0.95 | 0.95 |
| 6 | 0.96 | 0.96 | 0.96 |
| 7 | 0.95 | 0.96 | 0.95 |

## 3.2 ANN Model Performance

Table 3 shows the error evaluation of the four versions and Fig. 2 illustrates the scatter plot of actual and predicted values for the four ANN versions. The 45-degree line represents the ideal behavior of the model, with a 20% deviation indicated by the additional lines. The first version, using only geometric parameters, yielded less accurate and more conservative predictions compared to the others. The second version (with slenderness ratios), produced more scattered errors, especially for WB, exhibiting the highest MAPE (22.24%). The third version, which combines both geometric and slenderness parameters, on the other hand, exhibited the best performance, with the lowest MAPE (3.879%). The fourth version, which included the moment of inertia about the x-axis, showed a slight decline compared to the third version. Overall, all versions exhibited conservative results, with predicted values lower than those obtained by FEM, reinforcing the models' tendency to favor structural safety.

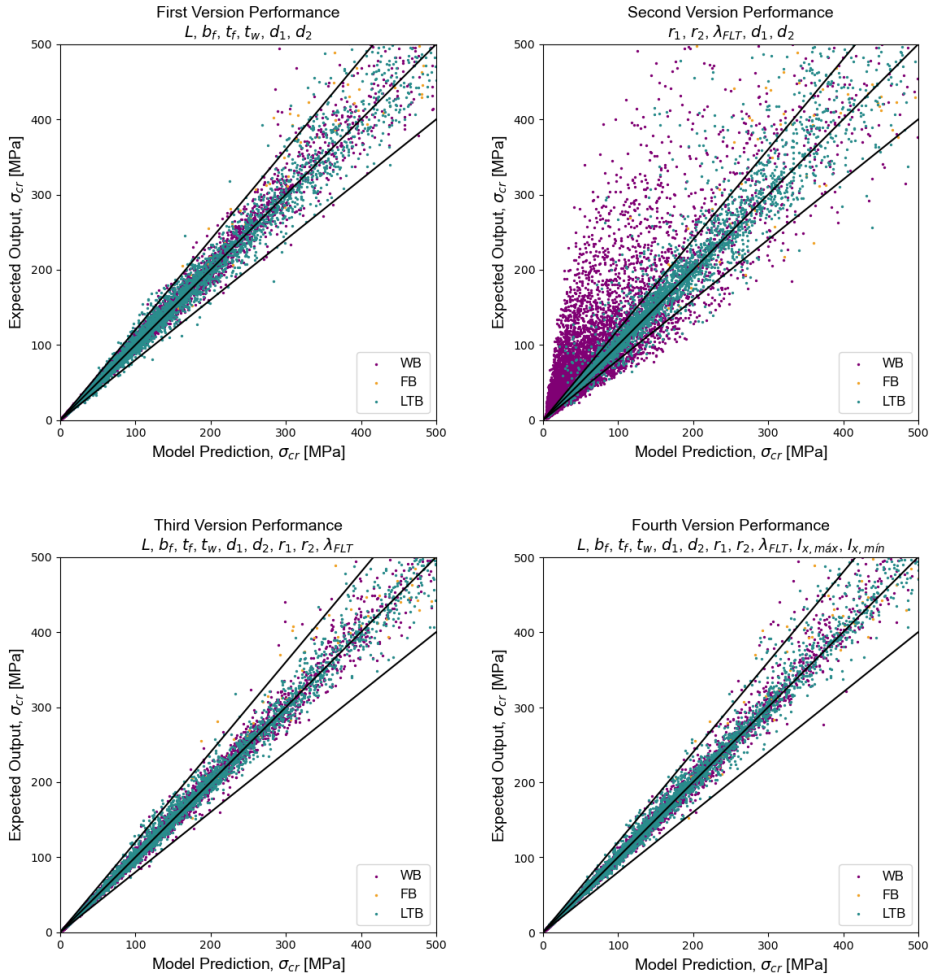



Figure 2. Scatter plot of actual and predicted values for the four ANN versions. The third version achieved the best agreement with the ideal model behavior, exhibiting the lowest MAPE (3.879%).

Table 3. Performance of the 4 versions of the 83/83/83/1 architecture

| Version | MAE [MPa] | MSE [MPa²] | MAPE [%] |
|---|---|---|---|
| 1 | 1.027E+01 | 1.367E+03 | 5.933E+00 |
| 2 | 2.629E+01 | 3.048E+03 | 2.224E+01 |
| 3 | 6.659E+00 | 5.085E+02 | 3.879E+00 |
| 4 | 7.537E+00 | 6.882E+02 | 4.102E+00 |

Table 4. Performance of third and fourth versions of the 83/83/83/1 architecture – Critical bending stress vs. critical bending moment prediction

| Version | Output | Unit | MAE | MSE | MAPE |
|---|---|---|---|---|---|
| 3 | $\sigma_{cr}$ | MPa | 6.659E+00 | 5.085E+02 | 3.879E+00 |
| | $M_{cr}$ | kN.m | 7.264E+01 | 3.495E+05 | 3.631E+00 |
| 4 | $\sigma_{cr}$ | MPa | 7.537E+00 | 6.882E+02 | 4.102E+00 |
| | $M_{cr}$ | kN.m | 6.452E+01 | 2.537E+05 | 3.633E+00 |

For the third and fourth versions, which demonstrated the best performances among the models, the ANNs were adjusted to predict the critical bending stress in beams instead of the critical bending moment. Table 4 exhibits comparative results obtained for both outputs. Although the model with critical bending stress prediction presented

a slightly better performance, the use of different outputs did not significantly impact the results. Thus, the stress-based model is recommended, given that it was trained using only four cross section depths, and the stresses are independent of the absolute beams' dimensions. The critical bending moment prediction may lead to higher errors if new depths are used.

Since the third version achieved the best performance, it was used as the baseline model for developing the class-specific ANNs. For the FB class, it was necessary to modify the ANN architecture from 83 neurons per layer to 10 neurons per layer, as this category has significantly less data available for training.

### 3.3 Effect of Data Classification on the Regression Model

Table 5 shows the performance of the standard and class-specific regression models. All classes demonstrated reduced predictive ability after data classification. This may be due to the fact that the hyperparameter tuning was applied to the conventional regression model only, which could compromise the performance of the class-specific ANNs, especially for the FB class, which had limited amount of training data.

Table 5. Performance of the standard and class-specific regression models

| Version | Output | Unit | MAE | MSE | MAPE |
|---|---|---|---|---|---|
| Standard | $\sigma_{cr}$ | MPa | 6.659E+00 | 5.085E+02 | 3.879E+00 |
| | $M_{cr}$ | kN.m | 7.264E+01 | 3.495E+05 | 3.631E+00 |
| Applied to WB | $\sigma_{cr}$ | MPa | 1.006E+01 | 9.082E+02 | 6.925E+00 |
| | $M_{cr}$ | kN.m | 6.063E+01 | 1.307E+05 | 3.627E+00 |
| Applied to FB | $\sigma_{cr}$ | MPa | 7.740E+01 | 1.201E+04 | 2.372E+01 |
| | $M_{cr}$ | kN.m | 2.623E+02 | 1.783E+05 | 4.153E+01 |
| Applied to LTB | $\sigma_{cr}$ | MPa | 2.153E+01 | 3.168E+03 | 8.871E+00 |
| | $M_{cr}$ | kN.m | 9.672E+01 | 2.258E+05 | 4.735E+00 |

### 3.4 Comparison Between the Regression Model and a Literature Formulation

The critical bending moment values obtained with the model were compared with values indicated by the formulation in [7]. Statistical parameters related to relative errors are exhibited in Tab. 6. The ANN model provided errors significantly smaller, which demonstrates the higher prediction capacity of these algorithms comparing to simpler literature formula. Braham and Hanikenne [7] formulation showed more conservative results, which may be due to its inconsideration of cross-sectional torsion stiffness.

Table 6. Relative error results - Proposed model vs. Braham and Hanikenne [7]

| Statistical parameter | Proposed model | Braham and Hanikenne |
|---|---|---|
| Maximum | 0.471095 | 7.133514 |
| Minimum | -0.334927 | -0.752085 |
| Mean | - 0.010834 | 0.317570 |
| MAPE | 0.03513 | 0.4099 |
| Standard Deviation | 0.050625 | 0.396109 |

## 4 Conclusions

This study showed that the proposed ANN model was capable of successfully predicting the LTB critical bending stress of web-tapered beams, with a MAPE of around 3%. The results demonstrate the effectiveness of such ML algorithms in developing complex regression models with relatively low errors. For design applications, the use of the model enables faster verification of design criteria and allows for a more adequate exploration of the full potential of web-tapered beams, as it prevents both over- and under-designed sections.

The inclusion of both geometric and slenderness features significantly increased the performance of the ANNs. However, including the moment of inertia about the x-axis feature leads to a slight decline in the ANNs'

predictive capability. Although the models that predict the critical bending moment showed better performance than the models that predict the critical bending stress, the latter are recommended since they do not depend on the absolute dimensions of the beam. In this way, for cases when the depth of the applied cross-section differs from those considered during training, the occurrence of errors is reduced. A considerable improvement was observed in predicting the critical moment with the model compared to the formulation in Braham and Hanikenne [7].

Future work should focus on studying other loadings, boundary conditions, and geometries of web-tapered members. Another important direction is to adapt the ANN and the database in order to predict the resistant bending moment, taking into account bar plastification and instability.

**Acknowledgements.** The authors would like to acknowledge the support provided by the Fundação de Amparo à Pesquisa e Inovação do Espírito Santo (FAPES), which made this research possible. The first author thanks FAPES for the research grant provided.

**Authorship statement.** The authors hereby confirm that they are the sole liable persons responsible for the authorship of this work, and that all material that has been herein included as part of the present paper is either the property (and authorship) of the authors, or has the permission of the owners to be included here.

## References

[1] R. D. Ziemian. *Guide to Stability Design Criteria for Metal Structures*. 6th ed., John Wiley & Sons, 2010.
[2] R. C. Kaehler, D. W. White, and Y. D. Kim. *Frame Design Using Web-Tapered Members*. American Institute of Steel Construction, Chicago, IL, USA, 2011.
[3] ABNT. *ABNT NBR 8800: Design of Steel Structures and Composite Steel-Concrete Structures for Buildings*. ABNT, Rio de Janeiro, 2024.
[4] EUROCODE 3. *EN 1993-1-1: Design of Steel Structures – Part 1-1: General Rules and Rules for Buildings*. Belgium, 2005.
[5] ANSI/AISC. *ANSI/AISC 360-22: Specification for Structural Steel Buildings*. AISC, 2022.
[6] M. A. Bradford, "Stability of tapered I-beams". *Journal of Constructional Steel Research*, vol. 9, no. 3, pp. 195–216, 1988.
[7] M. Braham and D. Hanikenne, "Lateral buckling of web tapered beams: An original design method confronted with a computer simulation". *Journal of Constructional Steel Research*, vol. 27, no. 1–3, pp. 23–36, 1993.
[8] Y. B. Yang and J. D. Yau, "Stability of beams with tapered I-sections". *Journal of Engineering Mechanics*, vol. 113, no. 9, pp. 1337–1357, 1987.
[9] H. Chen, Y. Liu, Y. Huang, J. Huang, L. Caisong, and Z. Guo, "Maximum displacement prediction model for steel beams with hexagonal web openings under impact loading based on artificial neural networks". *Engineering Applications of Artificial Intelligence*, vol. 136, p. 108932, 2024.
[10] V. M. Oliveira, A. S. Carvalho, A. Rossi, M. Hosseinpour, Y. Sharifi, and C. H. Martins, "Data-driven design approach for the lateral-distortional buckling in steel-concrete composite cellular beams using machine learning models". *Structures*, Elsevier, 2024, p. 106018.
[11] G. Hajdú, N. Bektaş, and A. Müller, "Machine learning models for the elastic-critical buckling moment of sinusoidal corrugated web beam". *Results in Engineering*, vol. 23, p. 102371, 2024.
[12] Q. Liu, X. Wang, Z. Guan, and Z. Li, "Rapid prediction and parameter evaluation of process-induced deformation in L-shape structures based on feature selection and artificial neural networks". *Journal of Composites Science*, vol. 8, no. 11, p. 455, 2024.
[13] L. Possidente and C. Couto, "Explained fire resistance machine learning models for compressed steel members of trusses and bracing systems". *Engineering Applications of Artificial Intelligence*, vol. 139, p. 109571, 2025.
[14] I. G. Raftoyiannis and T. Adamakos, "Critical lateral-torsional buckling moments of steel web-tapered I-beams". *The Open Construction & Building Technology Journal*, vol. 4, no. 1, 2010.
[15] M. Kováč, "Lateral-torsional buckling of web-tapered I-beams. 1D and 3D FEM approach". *Procedia Engineering*, vol. 40, pp. 217–222, 2012.
[16] B. Asgarian, M. Soltani, and F. Mohri, "Lateral-torsional buckling of tapered thin-walled beams with arbitrary cross-sections". *Thin-Walled Structures*, vol. 62, pp. 96–108, 2013.
[17] N. S. Trahair, "Interaction buckling of tapered beams". *Engineering Structures*, vol. 62, pp. 174–180, 2014.
[18] C. Couto, "Neural network models for the critical bending moment of uniform and tapered beams". *Structures*, Elsevier, 2022, pp. 1746–1762.
[19] D. P. Kingma and J. L. Ba, "ADAM: A method for stochastic optimization". *International Conference on Learning Representations (ICLR)*, San Diego, 2015. Available: https://arxiv.org/abs/1412.6980. Accessed: Feb. 27, 2025.